

**Fluorescence Resonance Energy Transfer–Based Analysis of cAMP Dynamics in Live Neonatal Rat Cardiac Myocytes Reveals Distinct Functions of Compartmentalized Phosphodiesterases**

Marco Mongillo, Theresa McSorley, Sandrine Evellin, Arvind Sood, Valentina Lissandron, Anna Terrin, Elaine Huston, Annette Hannawacker, Martin J. Lohse, Tullio Pozzan, Miles D. Houslay and Manuela Zaccolo

*Circulation Research* 2004, 95:67-75: originally published online June 3, 2004  
doi: 10.1161/01.RES.0000134629.84732.11

Circulation Research is published by the American Heart Association, 7272 Greenville Avenue, Dallas, TX 75214

Copyright © 2004 American Heart Association. All rights reserved. Print ISSN: 0009-7330. Online ISSN: 1524-4571

The online version of this article, along with updated information and services, is located on the World Wide Web at:

<http://circres.ahajournals.org/content/95/1/67>

Subscriptions: Information about subscribing to *Circulation Research* is online at  
<http://circres.ahajournals.org/subscriptions/>

Permissions: Permissions & Rights Desk, Lippincott Williams & Wilkins, a division of Wolters Kluwer Health, 351 West Camden Street, Baltimore, MD 21202-2436. Phone: 410-528-4050. Fax: 410-528-8550. E-mail:  
[journalpermissions@lww.com](mailto:journalpermissions@lww.com)

Reprints: Information about reprints can be found online at  
<http://www.lww.com/reprints>

## Fluorescence Resonance Energy Transfer–Based Analysis of cAMP Dynamics in Live Neonatal Rat Cardiac Myocytes Reveals Distinct Functions of Compartmentalized Phosphodiesterases

Marco Mongillo, Theresa McSorley, Sandrine Evellin, Arvind Sood, Valentina Lissandron, Anna Terrin, Elaine Huston, Annette Hannawacker, Martin J. Lohse, Tullio Pozzan, Miles D. Houslay, Manuela Zaccolo

**Abstract**—Cardiac myocytes have provided a key paradigm for the concept of the compartmentalized cAMP generation sensed by AKAP-anchored PKA. Phosphodiesterases (PDEs) provide the sole route for degrading cAMP in cells and are thus poised to regulate intracellular cAMP gradients. PDE3 and PDE4 represent the major cAMP degrading activities in rat ventriculocytes. By performing real-time imaging of cAMP in situ, we establish the hierarchy of these PDEs in controlling cAMP levels in basal conditions and on stimulation with a  $\beta$ -adrenergic receptor agonist. PDE4, rather than PDE3, appears to be responsible for modulating the amplitude and duration of the cAMP response to beta-agonists. PDE3 and PDE4 localize to distinct compartments and this may underpin their different functional roles. Our findings indicate the importance of distinctly localized PDE isoenzymes in determining compartmentalized cAMP signaling. (*Circ Res.* 2004;95:67-75.)

**Key Words:** phosphodiesterase ■ cAMP ■ heart signaling ■ fluorescence resonance energy transfer imaging

CAMP is known to modulate a variety of cellular functions such as carbohydrate metabolism, differentiation, and heart beating. cAMP is produced by adenylyl cyclases (AC) via stimulation of G protein-coupled receptors (GPCR), and its main effector is cAMP-dependent protein kinase (PKA). It has been suggested that parallel and spatially segregated cAMP signaling pathways coexist within a cell.<sup>1,2</sup> In this, a key role is played by A kinase anchoring proteins, scaffolding proteins anchoring PKA to specific intracellular locations in proximity to modulators and targets.<sup>3</sup> The selective activation of individual “pools” of PKA requires that cAMP is made available in discrete compartments.<sup>4</sup>

Cardiac cells, in which cAMP is a key regulator of excitation–contraction coupling, have played a pivotal role in developing this concept<sup>1,5,6</sup> for which direct experimental evidence has recently been provided.<sup>7,8</sup>

The level of cAMP in cells is the result of a balance between synthesis and degradation. In most studies the focus is given to GPCR regulation.<sup>9,10</sup> However, cAMP phosphodiesterases (PDEs) provide the only known route for degrading cAMP, uniquely positioning them to provide a

key regulatory role.<sup>5</sup> Members of the panoply of PDEs can be targeted to specific subcellular sites<sup>11</sup> and interact with anchor/scaffold proteins, including A kinase anchoring proteins.<sup>12,13</sup> PDEs are grouped in a superfamily, of which 8 families hydrolyze cAMP.<sup>5,11</sup> Their species-conserved diversity suggests that different isoforms play specific roles and, indeed, lack of redundancy in the PDE4 subfamily has been inferred from gene knockout studies.<sup>14</sup> PDEs differ not only in terms of intracellular targeting but also in activity,  $K_m$ , modulation, and expression.<sup>5</sup> PDEs are ideally suited to fix the boundaries for cAMP diffusion and thereby modulate defined sets of PKA-mediated events.<sup>1,7,8,15</sup> Although PDE activity in cardiac myocytes has been studied in some detail,<sup>16–18</sup> the contribution of individual PDE families in shaping the cAMP response to specific stimuli remains largely to be determined.

By directly measuring cAMP, we dissect the role of particular PDE families in the control of cAMP concentration in basal conditions and on  $\beta$ -AR stimulation, and provide direct evidence for distinct roles of PDE3 and PDE4 in forming and shaping cAMP transients in cardiomyocytes.

Original received February 13, 2004; revision received May 24, 2004; accepted May 25, 2004.

From the Dulbecco Telethon Institute (M.M., V.L., A.T., M.Z.), Venetian Institute of Molecular Medicine (M.M., S.E., V.L., T.P., M.Z.), Padova, Italy; Department of Biomedical Sciences (M.M., V.L., T.P.), University of Padova, Padova, Italy; Division of Biochemistry and Molecular Biology (T.M., A.S., E.H., M.D.H.), IBLS, Wolfson Building, University of Glasgow, Glasgow, Scotland; Institute of Pharmacology and Toxicology (A.H., M.J.L.), University of Würzburg, Würzburg, Germany.

Correspondence to Dr Manuela Zaccolo, Venetian Institute for Molecular Medicine, Room G210, Via Orus 2, Padova 35129, Italy. E-mail manuela.zaccolo@unipd.it

© 2004 American Heart Association, Inc.

*Circulation Research* is available at <http://www.circresaha.org>

DOI: 10.1161/01.RES.0000134629.84732.11

## Materials and Methods

### Chemicals and Reagents

Norepinephrine, rolipram, isobutyl-methyl-xanthine (IBMX), and cilostamide were from Sigma-Aldrich. Anti PDE3A antibody was from FabGennix Inc (Shreveport, La).

### Immunopurification of PDE4 Subfamilies for PDE Assay and Western Blots

This was performed as described before.<sup>19,20</sup> Briefly, insoluble proteins were removed from the lysate by centrifugation at 10 000g<sub>av</sub> for 20 minutes and the soluble fraction retained. The activity of individual PDE4 subfamilies was determined as before by quantitative immunopurification using specific antisera,<sup>19,20</sup> except here a rodent PDE4A-specific antisera<sup>20,21</sup> was used to immunopurify PDE4A. Western blotting of PDE4 isoforms was performed as before using C-terminal directed antisera.<sup>22,23</sup>

### Phosphodiesterase Assay

PDE activity was assayed using a modification of the Thompson and Appleman 2-step procedure<sup>24</sup> as described.<sup>25</sup> Protein concentration was determined using the Bradford method.<sup>26</sup>

### Dominant-Negative PDE4

As described before,<sup>11</sup> mutation of aspartate to alanine in the catalytic site renders PDE4 catalytically inactive with a dominant-negative function. Here we used the catalytically inactive D556A-PDE4D5 and D392A-PDE4B2 constructs.

### Immunostaining and Confocal Imaging

Cells were costained with anti-PDE and anti-alpha actinin antibodies (Sigma). Alexa fluor 488-conjugated antimouse antibody and Alexa fluor 543-conjugated anti goat antibody (Molecular Probes, Eugene, Ore) were used as secondary antibodies. Confocal images were acquired with a Bio-Rad 2100MP confocal system.

### Fluorescence Resonance Energy Transfer Imaging

Primary cultures of cardiac ventricular myocytes from 1- to 2-day-old Sprague Dawley rats were prepared as described.<sup>27</sup> After transfection with C-YFP and RII-CFP,<sup>28</sup> cells were imaged on an inverted Olympus IX50 microscope, equipped with a cooled charge-coupled device camera (Sensicam QE), a software-controlled monochromator (TILL Photonics), and a beam-splitter optical device (Microimager). Images were acquired using a custom-made software and processed using ImageJ (Rasband). Fluorescence resonance energy transfer (FRET) changes were measured as changes in the 480 nm/535 nm fluorescence emission intensities on excitation at 430 nm. Cells were perfused with HEPES-buffered Ringer modified saline (1 mmol/L CaCl<sub>2</sub>) at room temperature (20°C to 22°C). Norepinephrine pulses were delivered by means of a software-controlled pressurized micropipette in proximity of the analyzed cell and loaded with a 1 μmol/L norepinephrine.

## Results

### PDE Activity in Homogenates of Rat Neonatal Cardiac Myocytes

Lysates of neonatal rat cardiac myocytes expressed cAMP PDE activity at a level of 102 ± 8 pmol min<sup>-1</sup> mg protein<sup>-1</sup> with 1 μmol/L cAMP as substrate (mean ± SD; n = 8). PDE3 and 4 are believed to provide the major cAMP PDE activity in rat myocytes.<sup>29</sup> We determined lysate PDE3 and PDE4 activities using the highly selective inhibitors, cilostamide (10 μmol/L) and rolipram (10 μmol/L),<sup>11,30,31</sup> respectively. Figure 1A shows that ≈90% of the activity is provided by these 2 families, with the activity of PDE4 being double that of PDE3. PDE4 comprises 4 subfamilies

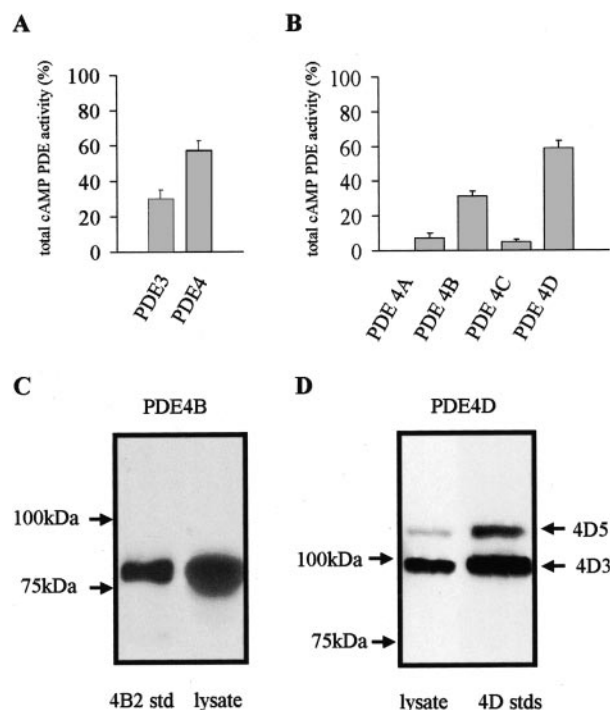


**Figure 1.** cAMP phosphodiesterase activity in neonatal cardiac myocytes. A, Cell lysates were assayed using 1 μmol/L cAMP as substrate. The PDE3 activity is denoted as that fraction of the total cAMP PDE activity inhibited by cilostamide (10 μmol/L) and the PDE4 activity the fraction inhibited by rolipram (10 μmol/L). Data are means ± SD of 6 experiments on different myocytes preparations. B, Selective immunoprecipitation of the 4 PDE4 subfamilies from myocytes and their relative PDE activity. The activity of each subfamily is expressed as a percentage of the total PDE4 activity. Data are means ± SD for 3 experiments. Immunopurification was performed using PDE4 subfamily-specific antisera (see Methods). C and D, Western blots using PDE4B- and PDE4D-specific antisera, respectively. Lysate protein (100 μg) was used against recombinant standards for (C) PDE4B2 and (D) PDE4D3 and PDE4D5. These blots are typical and were performed at least 3 times.

with various isoforms.<sup>11</sup> Using antisera that identify all isoforms within a particular subfamily,<sup>19,20</sup> we immunopurified each PDE4 subfamily for PDE assay. PDE4D and PDE4B together provide ≈90% of the total PDE4 activity, with PDE4D activity being double that of PDE4B, whereas PDE4A and PDE4C contribute <10% of total PDE4 activity (Figure 1B). Western blotting of lysates with specific antisera identified a single band comigrating with the short-form PDE4B2 recombinant standard (Figure 1C) and 2 bands comigrating with the long-form PDE4D3 and PDE4D5 recombinant standards (Figure 1D). The expression level of PDE4D3 was considerably greater than that of PDE4D5.<sup>12,32</sup>

### Individual PDE Families Play a Different Role in the Control of [cAMP]<sub>i</sub> in Resting Cardiomyocytes

The genetically encoded sensor for cAMP levels we developed<sup>8,28</sup> is based on FRET between a donor (CFP) and an acceptor fluorophore (YFP) fused to the regulatory (R) and catalytic (C) subunits of PKA, respectively. With this sensor, changes in cAMP concentration ([cAMP]<sub>i</sub>) can be estimated

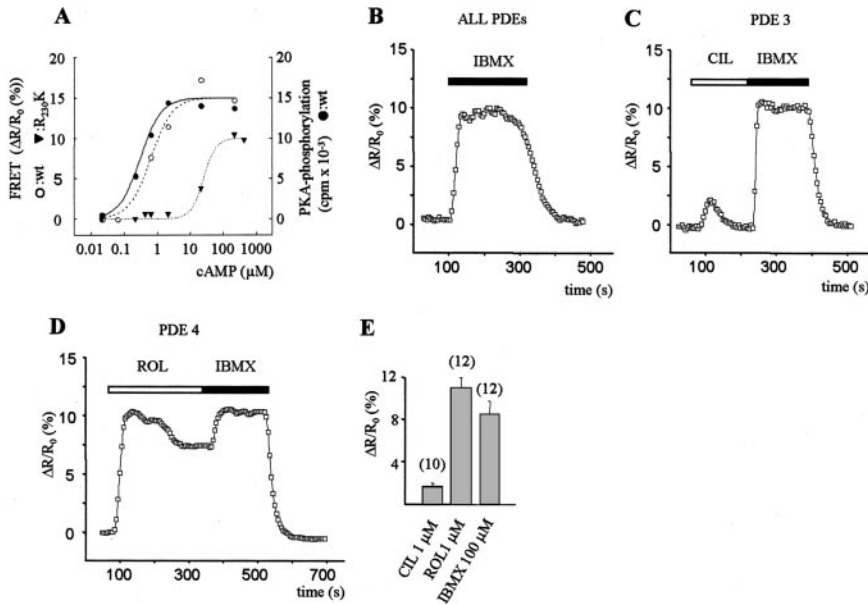


**Figure 2.** Effect of PDE inhibition on cAMP accumulation in unstimulated cells. A, cAMP dose-response curves measured as FRET changes of the wild-type (white circles) and R230K mutant probes (triangles) and kemptide phosphorylation (black circles). Kemptide phosphorylation assay was performed as described.<sup>50</sup> Lines were fitted to the Hill equation. Hill values are 1.4 ( $n=5$ ) for wild-type probe FRET; 1.7 ( $n=3$ ) for R230K mutant FRET; and 1.4 ( $n=8$ ) for kemptide phosphorylation. Representative plot of the effect on cAMP accumulation of IBMX (100  $\mu\text{mol/L}$ ) (B), cilostamide (1  $\mu\text{mol/L}$ ) (C), and rolipram (1  $\mu\text{mol/L}$ ) (D). The summary of the experiments performed in the conditions (B to D) is shown in (E). Number of cells analyzed is reported in brackets. Error bars indicate SEM.

by changes in FRET measured as changes in the CFP-to-YFP emissions ratio (480 nm/545 nm), a value that is proportional to  $[\text{cAMP}]_i$ . Figure 2A shows the cAMP-dependence of the probe in vitro as compared with its ability to phosphorylate the PKA peptide substrate Kemptide. The 2 assays gave identical  $\text{EC}_{50}$  values ( $\approx 0.3 \mu\text{mol/L}$ ).

Changes in FRET were expressed as the percent 480 nm/545 nm emission increase over the 480 nm/545 nm value at time 0 seconds ( $\Delta\text{R}/\text{R}_0$ ).

As mentioned previously,<sup>8</sup> treatment of the myocytes with a saturating (100  $\mu\text{mol/L}$ ) dose of the nonselective PDE inhibitor, IBMX, induces a maximal response ( $\Delta\text{R}/\text{R}_0$  of  $9 \pm 1.2\%$ , mean  $\pm$  SEM;  $n=10$ ) (Figure 2B and 2E) because no further increase was caused by subsequent addition of a saturating concentration (50  $\mu\text{mol/L}$ ) of the nonselective AC activator forskolin<sup>33</sup> (not shown). The velocity of the  $[\text{cAMP}]_i$  increase measured as  $(\Delta\text{R}/\text{R}_0)/\text{second}$  was  $0.17 \pm 0.03\%/ \text{second}$  ( $n=10$ ).

We focused on evaluating the effects of selectively inhibiting the major PDE activities, PDE3 and PDE4. As a control, IBMX (100  $\mu\text{mol/L}$ ) was used to inhibit both PDEs. PDE3 inhibition with cilostamide (1  $\mu\text{mol/L}$ ) increased  $[\text{cAMP}]_i$  with a  $\Delta\text{R}/\text{R}_0$  of  $1.7 \pm 0.4\%$  and a  $(\Delta\text{R}/\text{R}_0)/\text{second}$  of  $0.06 \pm 0.01\%/ \text{second}$  ( $n=10$ ) (Figure 2C and 2E). Cilostamide action was transient, with the signal returning back to the baseline by  $93 \pm 6$  seconds. In contrast, PDE4 inhibition with rolipram (1  $\mu\text{mol/L}$ ) generated a much larger ( $\Delta\text{R}/\text{R}_0 = 11.5 \pm 0.9\%$ ;  $n=12$ ) and faster [ $(\Delta\text{R}/\text{R}_0)/\Delta \text{seconds} = 0.25 \pm 0.03\%/ \text{seconds}$ ] increase of the signal (Figure 2D and 2E). In 40% of rolipram-treated cells, the increase in cAMP reached a sustained plateau, whereas in the remaining 60% the increase was partially reversible, reaching a plateau level at  $\approx 70\%$  of the peak 220  $\pm 50$  seconds after rolipram application (Figure 2D). These results indicate that PDE4 provides the major role in controlling  $[\text{cAMP}]_i$  under resting conditions.

### Action of PDE3 and PDE4 Inhibition on the $\beta$ -Adrenergic Receptor-Stimulated cAMP Response

Myocytes challenged with a submaximal (5 nmol/L) dose of the  $\beta$ -agonist norepinephrine generated a transient  $\Delta\text{R}/\text{R}_0 \approx 2\%$  over basal, returning to near initial levels in  $107 \pm 9.6$  seconds (Figure 3A and 3E). A subsequent addition of cilostamide caused a further increase in  $\Delta\text{R}/\text{R}_0$  of  $3.6 \pm 1.3\%$  ( $n=5$ ) (Figure 4A and 4E), with  $(\Delta\text{R}/\text{R}_0)/\text{second} = 0.06 \pm 0.01\%/ \text{second}$ . This increase was approximately twice that induced by cilostamide in unstimulated cells and was again transient ( $171 \pm 26.6$  seconds).

Inhibition of PDE4 with 1  $\mu\text{mol/L}$  rolipram causes a maximal response of the probe (Figure 2D and 2E). Thus, to assess the effect of PDE4 inhibition in norepinephrine-stimulated cells, we used a concentration (25 nmol/L) of rolipram that, in unstimulated conditions, exerts a minimal effect on  $[\text{cAMP}]_i$  (Figure 3B and 3E) and inhibits  $\approx 10\%$  of total PDE4 (Figure 3C). Under these conditions, 5 nmol/L norepinephrine causes (Figure 3D) a maximal and sustained response [ $\Delta\text{R}/\text{R}_0 = 9 \pm 2\%$ , and  $(\Delta\text{R}/\text{R}_0)/\text{second} = 0.05 \pm 0.01\%/ \text{second}$ ;  $n=5$ ].

The probe shows that PDE4 inhibition is profoundly more effective than PDE3 inhibition in potentiating norepinephrine-induced cAMP accumulation. We also examined total cAMP accumulation in myocytes using a radioimmunoassay. Inhibition of PDE4 with rolipram (1  $\mu\text{mol/L}$ ) was profoundly more effective than inhibition of PDE3 with cilostamide (1  $\mu\text{mol/L}$ ) on the ability of norepinephrine to increase cAMP levels (Figure 3F).

### Role of PDE3 and PDE4 Inhibition in Modulating the Duration of the cAMP Response to $\beta$ -Adrenergic Receptor Stimulation

PDE3 and PDE4 not only contribute differently to determine the amplitude of the cAMP response but also have different effects on the kinetics of this response, being transient subsequent to PDE3 inhibition yet sustained on PDE4 blockade (Figures 2C, 2D, 3A, and 3D). These

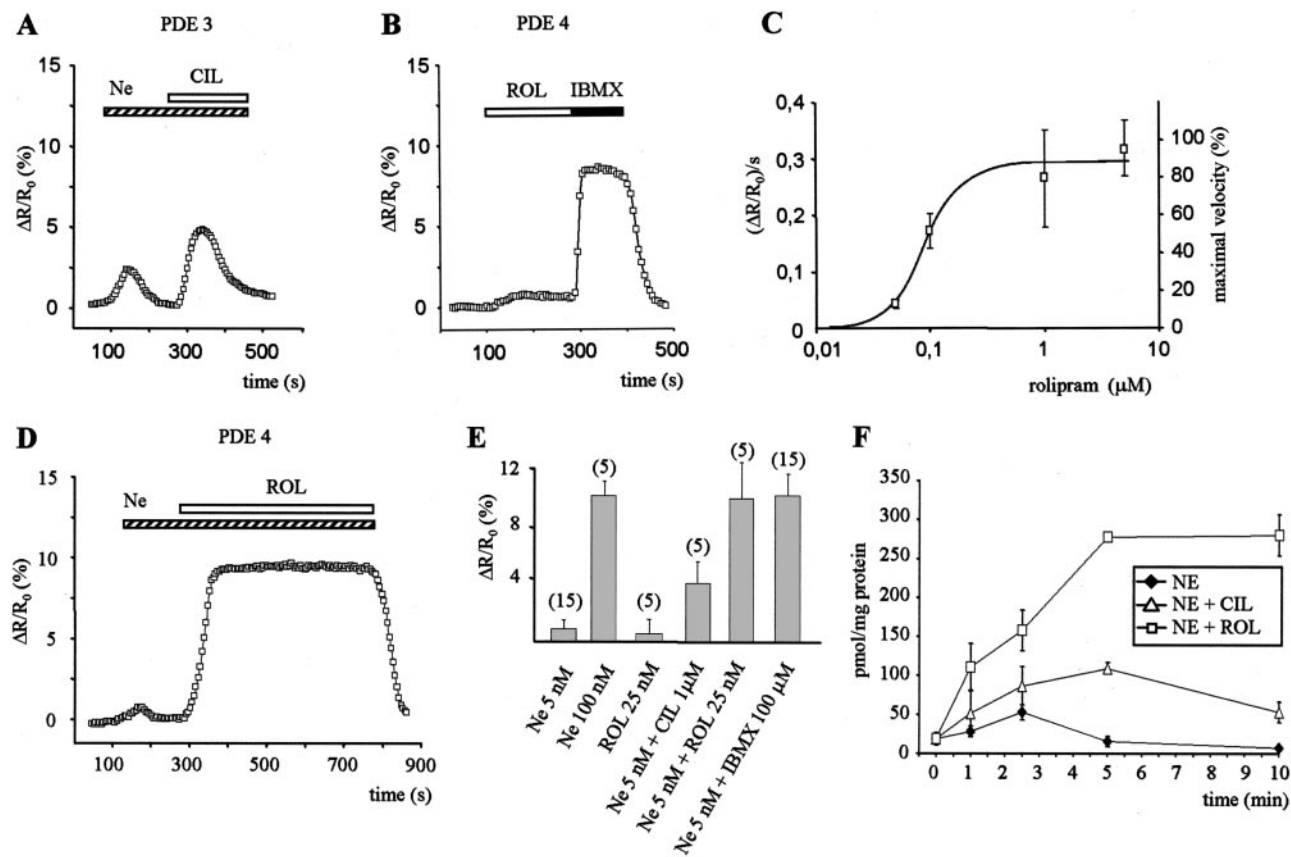


**Figure 3.** Effect of PDE inhibition on cAMP accumulation in cells stimulated with norepinephrine. Transfected cells were challenged with a submaximal dose (5 nmol/L) of norepinephrine and subsequently treated with a specific PDE inhibitor. Representative plot of the effect of 1  $\mu$ mol/L cilostamide (A) or 25 nmol/L rolipram (D) in the presence of 5 nmol/L norepinephrine and summary of the experiments performed in these conditions (E). B, Effect of 25 nmol/L rolipram alone is shown. C, Dose–response curve of rolipram-mediated FRET change. Response was calculated by measuring the velocity of 480 nm/535 nm emission increase in the first minute after the challenge with different rolipram concentrations. Each point is the average of 8 independent experiments in different cells. Bars indicate SEM. The solid line represents the best fitting, calculated with the least square method. A velocity of  $\approx 0.03\%$ /second can be extrapolated for 25 nmol/L rolipram that corresponds to approximately one-tenth the velocity elicited by 1  $\mu$ mol/L rolipram. F, Time course of cAMP accumulation as measured by radioimmunoassay on cell lysates. Norepinephrine was 1  $\mu$ mol/L, cilostamide was 1  $\mu$ mol/L, and rolipram was 1  $\mu$ mol/L (n=3 experiments).

distinct actions were confirmed in experiments in which myocytes were first treated with the indicated PDE inhibitor and subsequently challenged with a pulse (5 seconds) of a saturating concentration (1  $\mu$ mol/L) of norepinephrine. Figure 4A and 4B show that this norepinephrine pulse, administered in the presence of cilostamide, generated a response that was 1.5-fold higher than controls (norepinephrine alone), whereas the duration was indistinguishable ( $20 \pm 2.1$  seconds, n=8; Figure 4A and 4C) from controls. In contrast, treatment of cells with low concentrations (25 nmol/L) of rolipram generated a response that was not only 2-fold higher than controls (Figure 4A and 4B) but also considerably more sustained (time to half maximal decay  $78 \pm 9$  seconds, n=15) (Figure 4A and 4C). Thus, even in the presence of high concentrations of norepinephrine, PDE4 plays the key role in determining amplitude and duration of the cAMP response.

#### PDE4 Is Necessary and Sufficient for Terminating the cAMP Transient in Response to $\beta$ -Adrenergic Receptor Stimulation

To investigate whether PDE4 is primarily responsible for terminating the increase of  $[cAMP]_i$  in response to norepi-

nephrine, myocytes were challenged with  $\beta$ -agonist while perfused with high concentrations of rolipram (1  $\mu$ mol/L). Because complete PDE4 inhibition generates an increase in  $[cAMP]_i$  that is sufficient by itself, to saturate the probe (Figure 2D and 2E) we generated a variant of the sensor (R230K) with reduced cAMP sensitivity (unpublished data 2004).<sup>34</sup> This new probe detects cAMP levels that would completely saturate the wild-type sensor (compare Figure 5A with Figure 3E). For complete saturation of the R230K mutant probe, 100  $\mu$ mol/L IBMX plus 100 nmol/L norepinephrine are necessary (Figure 5A). The reduced sensitivity to cAMP of the R230K probe is confirmed by a higher ( $31.3 \pm 1.68 \mu$ mol/L) EC<sub>50</sub> value for dissociation as compared with the wild-type probe (Figure 2A). Treatment of myocytes expressing the R230K probe with 100 nmol/L norepinephrine in the presence of rolipram (1  $\mu$ mol/L) not only causes a further increase in  $[cAMP]_i$  ( $\Delta R/R_0 = 5.2 \pm 0.8\%$ , n=4) but also sustains it for at least 10 minutes (Figure 5B).

#### PDE3 and PDE4 Provide Distinct Functional Roles in Determining cAMP Levels

The different effects of PDE3 and PDE4 inhibitors on resting and  $\beta$ AR-induced increase of  $[cAMP]_i$  suggest that these 2

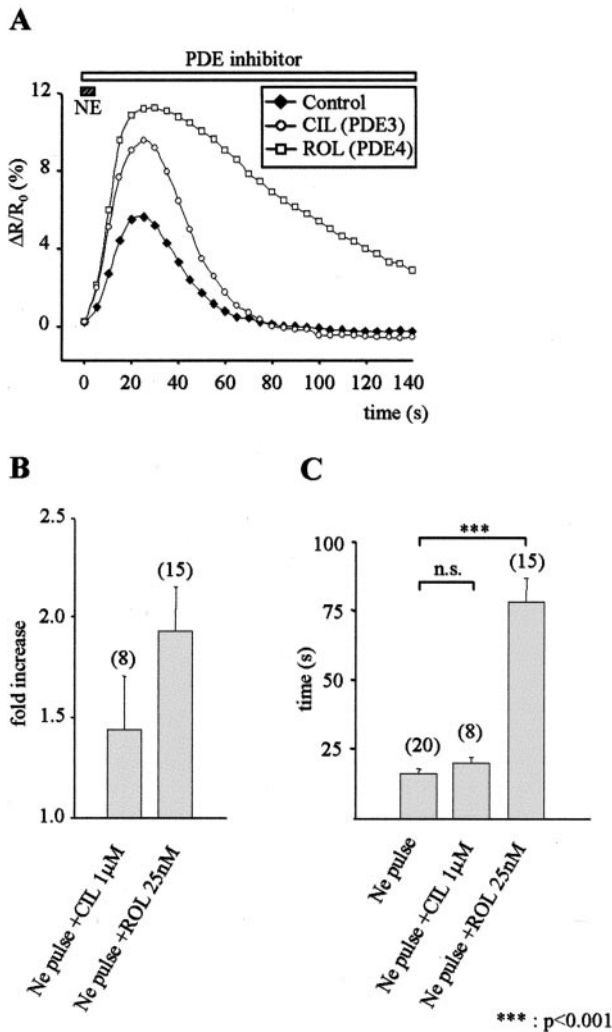


**Figure 4.** Effect of PDE inhibitors on the amplitude and duration of the cAMP transient elicited by a pulsed stimulation of the  $\beta$ -receptor. A, Increase in cAMP induced by a pulse of norepinephrine alone and in combination with selective inhibitors is shown. B, Summary of the effects of the PDE inhibitors on the peak amplitude and (C) duration of the cAMP transient, in cells stimulated as indicated. Duration of the response is calculated as the time required for half maximal decay from peak.

enzyme families may reside in distinct compartments. Thus, we assessed the effect of selective PDE inhibitors on the cAMP response in cells in which the entire AC pool was activated by forskolin.

As shown in Figure 6, treatment with low forskolin (100 nmol/L) alone generated a small response ( $\Delta R/R_0 = 1.05 \pm 0.39\%$ ;  $n = 10$ ). The subsequent addition of cilostamide (1  $\mu\text{mol/L}$ ) generated a marked increase in cAMP levels with a  $\Delta R/R_0$  of  $5.9 \pm 1.1\%$  ( $n = 5$ ) and a  $\Delta R/R_0/\text{second}$  of  $0.08 \pm 0.01\%$  (Figure 6A and 6C). Again, these were transient, returning to baseline in  $182 \pm 29$  seconds, compatible with PKA-mediated activation of PDE4.<sup>35</sup> Addition of 25 nmol/L rolipram to cells pretreated with low forskolin generated a sustained increase in signal with a  $\Delta R/R_0$  of  $3.7 \pm 1.2\%$  ( $n = 5$ ) and a  $\Delta R/R_0/\text{second}$  of  $0.04 \pm 0.01\%$  (Figure 6B and 6C). Thus, selective PDE inhibition generates strikingly different effects on

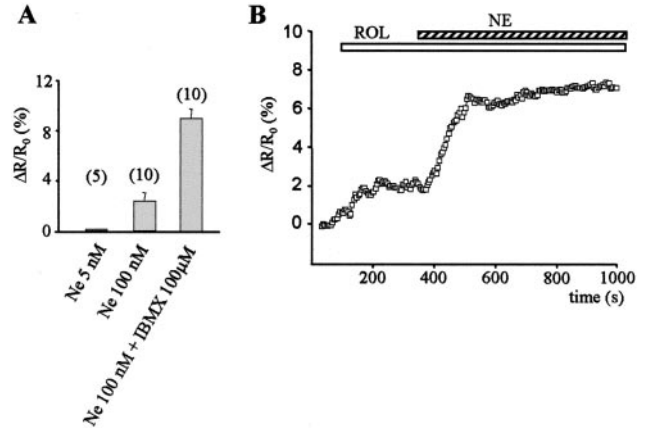


**Figure 5.** Role of PDE4 in regulating the cAMP increase induced by  $\beta$ -adrenergic stimulation or PDE3 inhibition. A, Sensitivity range of the R230K sensor measured by challenging transfected cells with different concentrations of norepinephrine and with a saturating stimulus (norepinephrine + IBMX). B, FRET change elicited by 100 nmol/L norepinephrine in cells transfected with the R230K sensor in which PDE4 activity was ablated by continuous treatment with 1  $\mu\text{mol/L}$  rolipram.

[cAMP]<sub>i</sub> when AC is activated by forskolin or via  $\beta$ -AR. In the presence of forskolin, rolipram enhanced  $\Delta R/R_0$  0.6 times compared with cilostamide, whereas with norepinephrine, rolipram amplified the response 2.2 times compared with cilostamide (Figure 6D). We attempted to estimate the size of the  $\beta$ -AR-sensitive pool of AC by transfecting myocytes with the R230K probe and comparing the cAMP response caused by saturating (10  $\mu\text{mol/L}$ ) norepinephrine or with the maximal cAMP response obtained in the presence of total AC activation (10  $\mu\text{mol/L}$  norepinephrine plus 25  $\mu\text{mol/L}$  forskolin). The pool of AC activated by norepinephrine is, at most,  $75 \pm 4\%$  ( $n = 5$ ) of the total ACs.

### Localization of PDE3 and PDE4 Families

Our results prompted us to investigate whether PDE3 and PDE4 may have distinct subcellular localizations using immunocytochemistry and confocal microscopy. PDE3A displayed nonhomogeneous trabecular staining (Figure 7A through 7D) compatible with localization on internal membranes. In contrast, both PDE4B and 4D Abs identified a low-signal granular pattern in the cytosol and a much stronger signal in a striated pattern (Figure 7E through 7I). The PDE4B signal intercalated with the striated pattern of  $\alpha$ -actinin, suggestive of localization to the sarcomeric M-line (Figure 7E through 7H), whereas PDE4D showed a striated pattern superimposable with that of  $\alpha$ -actinin, suggestive of localization to the Z-line (Figure 7I through 7L). PKA shows a striated pattern in correspondence to the M and Z lines (Figure 8M through 8P).

Knowledge of the 3-dimensional structure of the PDE catalytic unit has allowed catalytically inactive PDE4 isoforms to be generated by single point mutation.<sup>32</sup> Expression of such inactive PDE4 has been shown<sup>32</sup> to exert a dominant-negative effect by displacing the cognate endogenous, active PDE4 isoform from its functionally relevant anchor site and thus, presumably, allowing localized cAMP levels around such anchor sites to be raised. As an initial attempt to

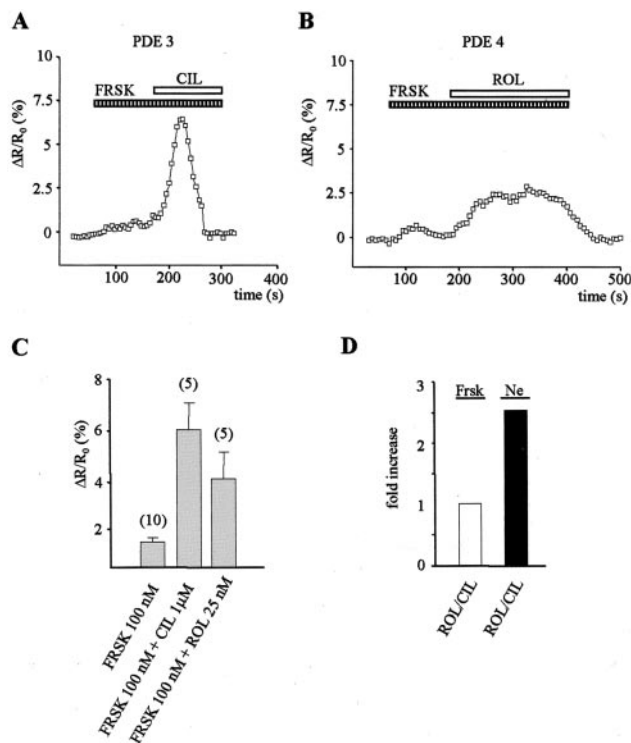


**Figure 6.** Effect of specific PDE inhibitors on cAMP accumulation in cells treated with forskolin. Representative plots of the cAMP response elicited by 1  $\mu$ M cilostamide (A) or 25 nmol/L rolipram (B), in cells previously challenged with a sub-maximal dose (100 nmol/L) of forskolin. A summary of all experiments performed in the different conditions is shown in (C). D, Effect of PDE4 inhibition versus PDE3 inhibition on cAMP concentration in the presence of 100 nmol/L forskolin (white bars) or 5 nmol/L norepinephrine (black bars) is compared.

determine if the different location of PDE4B and PDE4D confers a specific function to these 2 subfamilies, we measured the kinetics of cAMP response on challenge with a pulse (5 seconds) of 1  $\mu$ M norepinephrine in cells transfected with either dominant-negative PDE4B2 or dominant-negative PDE4D5, dominant-negative constructs. We detected a small but significant delay in the time required for the cAMP transient to return to baseline in cells expressing the dominant-negative PDE4B2 (time to half maximal decay =  $22.5 \pm 1.1$ ) as compared with either the control ( $15.8 \pm 1.2$ ) or the dominant-negative PDE4D5-expressing cells ( $19 \pm 2$ ) (Figure 8). Such delay was amplified when total endogenous PDE4 activity was partially inhibited with 25 nmol/L rolipram (time to half maximal decay  $107 \pm 11$  for PDE4B2 dominant-negative-expressing cells,  $72 \pm 6$  for control cells, and  $73 \pm 7$  for PDE4D5 dominant-negative-expressing cells). These results suggest that PDE4B2 plays a major role in the control of the duration of the cAMP transient in response to norepinephrine and that this function is dependent on its location within the cell.

### Discussion

Consistent with earlier studies,<sup>29,36</sup> PDE3 and PDE4 provide the major cAMP PDE activity in cardiac myocytes. PDEs from multiple gene families are invariably coexpressed within the same cell; however, much remains to be under-

stood as to how PDEs are engaged in the control of basal  $[cAMP]_i$  and changes in response to  $\beta$ AR stimulation. We exploit the high sensitivity and temporal resolution of the FRET-based imaging approach to measure real-time kinetics of PKA activation in the presence of physiological concentration of agonist, a measure difficult to obtain by radioimmunoassay.<sup>5</sup> PDE3 affinity for cAMP is known to be higher than that of PDE4;<sup>37</sup> therefore, PDE3 is thought to control cAMP levels in basal conditions.<sup>38</sup> However, the increase in  $[cAMP]_i$  was much smaller on inhibition of PDE3 than on inhibition of PDE4 (Figure 2C and 2D), indicating that basal AC activity in these cells is sufficient to keep  $[cAMP]_i$  at levels compatible with PDE4 affinity. PDE3 inhibition generates an increase in  $[cAMP]_i$ , which is transient, possibly because of PKA-mediated PDE4 activation<sup>31,35,39</sup> after the increase in cAMP generated by PDE3 inhibition. When myocytes are challenged with a PDE4 inhibitor, the increase in  $[cAMP]_i$  is stable, implying that the other PDEs acting together cannot compensate for the decreased PDE4 activity. This is despite indications that PDE3 can potentially be activated by PKA.<sup>30</sup>

We observed a striking difference between PDE3 and PDE4 inhibition in the control of  $[cAMP]_i$  on  $\beta$ AR stimulation. Thus, in the presence of norepinephrine, inhibition of  $\approx 10\%$  of total PDE4 (as obtained with 25 nM rolipram, Figure 3C), resulted in a dramatic increase in cAMP, whereas total PDE3 inhibition had only a marginal effect (Figure 3E). A similar difference was seen for changes in "bulk" cAMP determined immunochemically in cell lysates (Figure 3F). These data indicate a functional coupling of PDE4, rather than PDE3, with a pool of AC that is activated in response to  $\beta$ AR stimulation. In contrast, when the entire cellular pool of AC was stimulated with forskolin, complete inhibition of PDE3 had an effect that was now clearly greater than that caused by a partial inhibition of PDE4 (Figure 6). The fact that inhibition of only  $\approx 10\%$  of total PDE4 has such profound effect on the norepinephrine-generated cAMP transient suggests that compartmentation of PDEs may be equally important as their expression level.

We show that PDE4 has the potential to play a prominent role in regulating catecholamine-induced increases in  $[cAMP]_i$ . It will be interesting to see if this occurs in those species, including humans, in which, unlike rats, PDE4 does not represent the major quota of total PDE activity in heart tissue.<sup>40</sup> Considerable attention has been focused on the regulation of PDE3 in the development of cardiomyopathy, particularly heart failure.<sup>41</sup> PDE3 inhibitors were originally developed as therapeutic agents to counteract the reduced synthesis of cAMP found in failing hearts. However, trials with milrinone were interrupted because chronic treatment resulted in increased mortality.<sup>42</sup> The reasons for such adverse effects are still to be elucidated, but it is conceivable that they may in part have resulted from a nonselective elevation of cAMP in multiple compartments and indiscriminate activation of PKA<sup>43</sup> (milrinone can affect both PDE4 and PDE3).<sup>44</sup> Little, however, is known about the role for PDE4 in human heart pathology. Our data suggest that alterations in PDE4 activity may influence  $\beta$ AR signaling in the heart. Recent evidence<sup>45</sup> shows that  $\beta$ AR agonist can

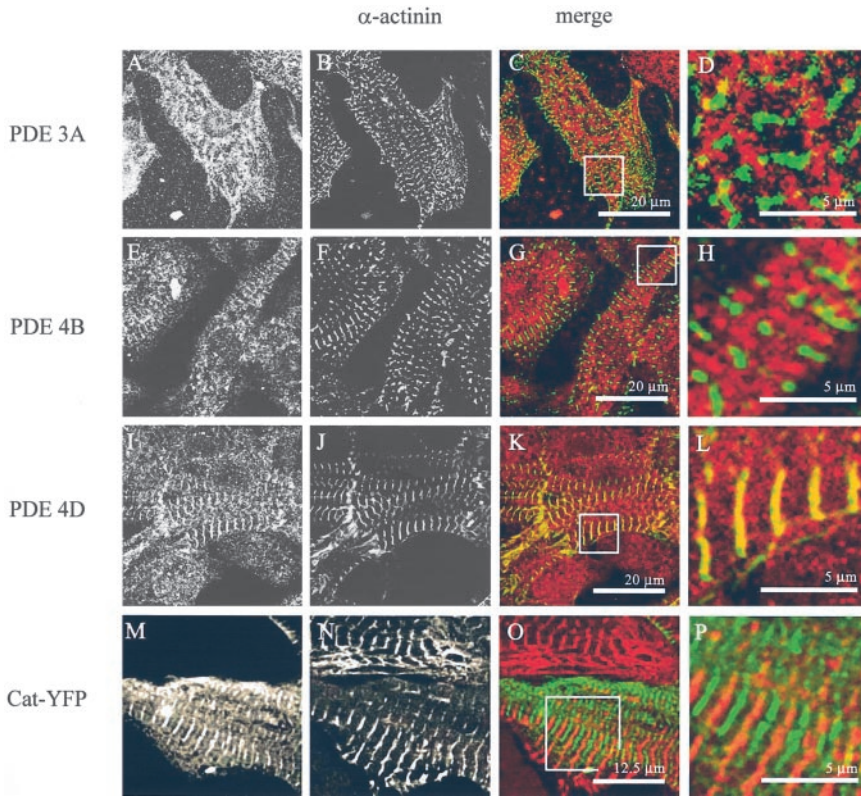


**Figure 7.** Subcellular localization of PDE3A, PDE4B, and PDE4D. Confocal images of PDE 3A (A), PDE 4B (E), and PDE 4D (I) localization in cultured cardiac myocytes from neonatal rat hearts. Myocytes were decorated with polyclonal anti-PDE antibodies and costained with a monoclonal anti- $\alpha$ -actinin antibody (B,F,J). D, H, and L, Magnification of the boxed area in C, G, and K, respectively. The confocal image of myocytes transfected with YFP-tagged catalytic subunit of PKA (C-YFP) (M) and costained with  $\alpha$ -actinin antibody (N) are overlaid in (O) and the enlarged inset is shown in (P).

cause PDE4D to be recruited to the  $\beta$ AR in complex with  $\beta$ -arrestin. Our data indicate that even a modest hyperactivity of PDE4 may result in an appreciable blunting of the cAMP response to catecholamines, whereas a reduced activity of PDE4 may lead to an exaggerated response in terms of amplitude and duration. Interestingly, an increase in PDE4 activity from 20% to 39% of the total PDE activity has been

documented in failing hearts in dogs.<sup>41</sup> It is tempting to speculate that an increased activity and/or a mistargeting of PDE4 enzymes may contribute to reduce the inotropic response to milrinone observed in severe heart failure.

PDEs have been suggested to contribute to the compartmentation of cAMP signaling.<sup>8,46</sup> In particular, a key role for PDE3 and PDE4 in limiting the diffusion of cAMP from the plasma membrane to the cytosol of frog ventriculocytes has been proposed.<sup>15</sup> Our data provide new insights to the concept of compartmentalized cAMP signaling and suggest a model whereby PDEs from distinct families independently and coordinately modulate  $[cAMP]_i$  in selected functional compartments. We propose that PDE4 is primarily associated with regulating cAMP emanating from the  $\beta$ AR-activated AC domain. That  $\beta$ AR agonist challenge causes the  $\beta$ -arrestin-mediated recruitment of PDE4 to  $\beta_2$ AR in rat cardiac myocytes<sup>45</sup> demonstrates that PDE4 and  $\beta$ AR can be physically coupled in this cell type. We have shown that PDE3 and PDE4 have distinct localization, consistent with earlier biochemical studies in cardiac tissue.<sup>47,48</sup> It is likely that such compartmentalization of cAMP signaling controlled by PDE3 and PDE4 will have functional consequences, and this is consistent with the different effects that selective inhibitors of these exert on various cell types.<sup>30</sup> Rolipram treatment of guinea pigs, despite increasing cAMP levels, is unable to alter the phosphorylation status of phospholamban and troponin I.<sup>49</sup>

In conclusion, the spatial confinement of different PDEs to discrete compartments and their functional coupling to individual receptors may provide an efficient way to control local levels of cAMP in a stimulus-specific manner. This prompts

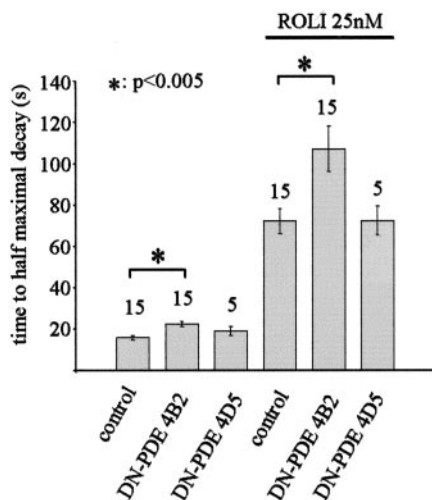


**Figure 8.** Effect of PDE4B2 and PDE4D5 dominant-negative proteins on the duration of the cAMP transient generated by a pulsed stimulation of  $\beta$ -receptor. Bars show the time required for half maximal decay from peak cAMP response in cells stimulated with a pulse (5 seconds) of norepinephrine. Cells were transfected with the cAMP probe alone (control), with PDE4B2 dominant-negative or with PDE4D5 dominant-negative constructs. Experiments were performed either in saline or in the presence of 25 nmol/L rolipram, as indicated.

the possibility of developing novel therapeutic approaches to correct cAMP imbalance in heart tissue.

### Acknowledgments

This work was supported by Telethon Italy (TCP00089), the Italian Cystic Fibrosis Research Foundation, and the Fondazione Compagnia di San Paolo (M.Z.); the European Union (QLK3-CT-2002-02149) (M.Z. and M.D.H.); the Medical Research Council (G8604010) and British Heart Foundation (FS/1999043) (M.D.H.); and Telethon, the Italian Association for Cancer Research, the Italian Ministry of Education, and the Italian Ministry of Health (T.P.).

### References

- Steinberg SF, Brunton LL. Compartmentation of G protein-coupled signaling pathways in cardiac myocytes. *Annu Rev Pharmacol Toxicol.* 2001;41:751–773.
- Zaccolo M, Magalhaes P, Pozzan T. Compartmentalisation of cAMP and Ca(2+) signals. *Curr Opin Cell Biol.* 2002;14:160–166.
- Colledge M, Scott JD. AKAPs: from structure to function. *Trends Cell Biol.* 1999;9:216–221.
- Laporte SA, Oakley RH, Caron MG. Signal transduction. *Bringing channels closer to the action!* *Science.* 2001;293:62–63.
- Beavo JA, Brunton LL. Cyclic nucleotide research—still expanding after half a century. *Nat Rev Mol Cell Biol.* 2002;3:710–718.
- Buxton IL, Brunton LL. Compartments of cyclic AMP and protein kinase in mammalian cardiomyocytes. *J Biol Chem.* 1983;258:10233–10239.
- Jurevicius J, Fischmeister R. cAMP compartmentation is responsible for a local activation of cardiac Ca<sup>2+</sup> channels by beta-adrenergic agonists. *Proc Natl Acad Sci U S A.* 1996;93:295–299.
- Zaccolo M, Pozzan T. Discrete microdomains with high concentration of cAMP in stimulated rat neonatal cardiac myocytes. *Science.* 2002;295:1711–1715.
- Kohout TA, Lefkowitz RJ. Regulation of G protein-coupled receptor kinases and arrestins during receptor desensitization. *Mol Pharmacol.* 2003;63:9–18.
- Lohse MJ, Engelhardt S, Eschenhagen T. What is the role of beta-adrenergic signaling in heart failure? *Circ Res.* 2003;93:896–906.
- Houslay MD, Adams DR. PDE4 cAMP phosphodiesterases: modular enzymes that orchestrate signalling cross-talk, desensitization and compartmentalization. *Biochem J.* 2003;370:1–18.
- Dodge KL, Khouangsathiene S, Kapiloff MS, Mouton R, Hill EV, Houslay MD, Langeberg LK, Scott JD. mA KAP assembles a protein kinase A/PDE4 phosphodiesterase cAMP signaling module. *Embo J.* 2001;20:1921–1930.
- Tasken KA, Collas P, Kemmner WA, Witczak O, Conti M, Tasken K. Phosphodiesterase 4D and protein kinase a type II constitute a signaling unit in the centrosomal area. *J Biol Chem.* 2001;276:21999–22002.
- Haraguchi T, Shimi T, Koujin T, Hashiguchi N, Hiraoka Y. Spectral imaging fluorescence microscopy. *Genes Cells.* 2002;7:881–887.
- Jurevicius J, Skeberdis VA, Fischmeister R. Role of cyclic nucleotide phosphodiesterase isoforms in cAMP compartmentation following beta<sub>2</sub>-adrenergic stimulation of IC<sub>a,L</sub> in frog ventricular myocytes. *J Physiol.* 2003;551:239–252.
- Bode DC, Kanter JR, Brunton LL. Cellular distribution of phosphodiesterase isoforms in rat cardiac tissue. *Circ Res.* 1991;68:1070–1079.
- Picq M, Dubois M, Grynberg A, Lagarde M, Prigent AF. Developmental differences in distribution of cyclic nucleotide phosphodiesterase isoforms in cardiomyocytes and the ventricular tissue from newborn and adult rats. *J Cardiovasc Pharmacol.* 1995;26:742–750.
- Verde I, Vandecasteele G, Lezoualc'h F, Fischmeister R. Characterization of the cyclic nucleotide phosphodiesterase subtypes involved in the regulation of the L-type Ca<sup>2+</sup> current in rat ventricular myocytes. *Br J Pharmacol.* 1999;127:65–74.
- MacKenzie SJ, Yarwood SJ, Peden AH, Bolger GB, Vernon RG, Houslay MD. Stimulation of p70S6 kinase via a growth hormone-controlled phosphatidylinositol 3-kinase pathway leads to the activation of a PDE4A cyclic AMP-specific phosphodiesterase in 3T3-F442A preadipocytes. *Proc Natl Acad Sci U S A.* 1998;95:3549–3554.
- MacKenzie SJ, Houslay MD. Action of rolipram on specific PDE4 cAMP phosphodiesterase isoforms and on the phosphorylation of cAMP-response-element-binding protein (CREB) and p38 mitogen-activated protein (MAP) kinase in U937 monocytic cells. *Biochem J.* 2000;347:571–578.
- McPhee I, Pooley L, Lobban M, Bolger G, Houslay MD. Identification, characterization and regional distribution in brain of RPDE-6 (RNPDE4A5), a novel splice variant of the PDE4A cyclic AMP phosphodiesterase family. *Biochem J.* 1995;310:965–974.
- Shepherd M, McSorley T, Olsen AE, Johnston LA, Thomson NC, Baillie GS, Houslay MD, Bolger GB. Molecular cloning and subcellular distribution of the novel PDE4B4 cAMP-specific phosphodiesterase isoform. *Biochem J.* 2003;370:429–438.
- Bolger GB, Erdogan S, Jones RE, Loughney K, Scotland G, Hoffmann R, Wilkinson I, Farrell C, Houslay MD. Characterization of five different proteins produced by alternatively spliced mRNAs from the human cAMP-specific phosphodiesterase PDE4D gene. *Biochem J.* 1997;328:539–548.
- Thompson WJ, Appleman MM. Multiple cyclic nucleotide phosphodiesterase activities from rat brain. *Biochemistry.* 1971;10:311–316.
- Marchmont RJ, Houslay MD. A peripheral and an intrinsic enzyme constitute the cyclic AMP phosphodiesterase activity of rat liver plasma membranes. *Biochem J.* 1980;187:381–392.
- Bradford MM. A rapid and sensitive method for the quantitation of microgram quantities of protein utilizing the principle of protein-dye binding. *Anal Biochem.* 1976;72:248–254.
- Dostal DE, Rothblum KN, Conrad KM, Cooper GR, Baker KM. Detection of angiotensin I and II in cultured rat cardiac myocytes and fibroblasts. *Am J Physiol.* 1992;263:C851–C863.
- Zaccolo M, De Giorgi F, Cho CY, Feng L, Knapp T, Negulescu PA, Taylor SS, Tsien RY, Pozzan T. A genetically encoded, fluorescent indicator for cyclic AMP in living cells. *Nat Cell Biol.* 2000;2:25–29.
- Takahashi K, Osanai T, Nakano T, Wakui M, Okumura K. Enhanced activities and gene expression of phosphodiesterase types 3 and 4 in pressure-induced congestive heart failure. *Heart Vessels.* 2002;16:249–256.
- Manganiello VC, Degerman E. Cyclic nucleotide phosphodiesterases (PDEs): diverse regulators of cyclic nucleotide signals and inviting molecular targets for novel therapeutic agents. *Thromb Haemost.* 1999;82:407–411.
- Conti M, Richter W, Mehats C, Livera G, Park JY, Jin C. Cyclic AMP-specific PDE4 phosphodiesterases as critical components of cyclic AMP signaling. *J Biol Chem.* 2003;278:5493–5496.
- Baillie GS, Sood A, MCPhee I, Gall I, Perry SJ, Lefkowitz RJ, Houslay MD. beta-Arrestin-mediated PDE4 cAMP phosphodiesterase recruitment regulates beta-adrenoceptor switching from G<sub>s</sub> to G<sub>i</sub>. *Proc Natl Acad Sci U S A.* 2003;100:940–945.
- Smit MJ, Iyengar R. Mammalian adenylyl cyclases. *Adv Second Messenger Phosphoprotein Res.* 1998;32:1–21.
- Hemmer W, McGlone M, Taylor SS. Recombinant strategies for rapid purification of catalytic subunits of cAMP-dependent protein kinase. *Anal Biochem.* 1997;245:115–122.
- Oki N, Takahashi SI, Hidaka H, Conti M. Short term feedback regulation of cAMP in FRTL-5 thyroid cells. Role of PDE4D3 phosphodiesterase activation. *J Biol Chem.* 2000;275:10831–10837.
- Wechsler J, Choi YH, Krall J, Ahmad F, Manganiello VC, Movsesian MA. Isoforms of cyclic nucleotide phosphodiesterase PDE3A in cardiac myocytes. *J Biol Chem.* 2002;277:38072–38078.
- Degerman E, Belfrage P, Manganiello VC. Structure, localization, and regulation of cGMP-inhibited phosphodiesterase (PDE3). *J Biol Chem.* 1997;272:6823–6826.
- Beavo JA. Cyclic nucleotide phosphodiesterases: functional implications of multiple isoforms. *Physiol Rev.* 1995;75:725–748.
- Baillie GS, MacKenzie SJ, MCPhee I, Houslay MD. Sub-family selective actions in the ability of Erk2 MAP kinase to phosphorylate and regulate the activity of PDE4 cyclic AMP-specific phosphodiesterases. *Br J Pharmacol.* 2000;131:811–819.
- Movsesian MA, Smith CJ, Krall J, Bristow MR, Manganiello VC. Sarcoplasmic reticulum-associated cyclic adenosine 5'-monophosphate phosphodiesterase activity in normal and failing human hearts. *J Clin Invest.* 1991;88:15–19.
- Smith CJ, Huang R, Sun D, Ricketts S, Hoegler C, Ding JZ, Moggio RA, Hintze TH. Development of decompensated dilated cardiomyopathy is associated with decreased gene expression and activity of the milrinone-sensitive cAMP phosphodiesterase PDE3A. *Circulation.* 1997;96:3116–3123.
- Parker I, Yao Y. Regenerative release of calcium from functionally discrete subcellular stores by inositol trisphosphate. *Proc R Soc Lond B Biol Sci.* 1991;246:269–274.

43. Movsesian MA. Beta-adrenergic receptor agonists and cyclic nucleotide phosphodiesterase inhibitors: shifting the focus from inotropy to cyclic adenosine monophosphate. *J Am Coll Cardiol.* 1999;34:318–324.
44. Shakur Y, Fong M, Hensley J, Cone J, Movsesian MA, Kambayashi J, Yoshitake M, Liu Y. Comparison of the effects of cilostazol and milrinone on cAMP-PDE activity, intracellular cAMP and calcium in the heart. *Cardiovasc Drugs Ther.* 2002;16:417–427.
45. Perry SJ, Baillie GS, Kohout TA, McPhee I, Magiera MM, Ang KL, Miller WE, McLean AJ, Conti M, Houslay MD, Lefkowitz RJ. Targeting of cyclic AMP degradation to beta 2-adrenergic receptors by beta-arrestins. *Science.* 2002;298:834–836.
46. Rich TC, Fagan KA, Tse TE, Schaack J, Cooper DM, Karpen JW. A uniform extracellular stimulus triggers distinct cAMP signals in different compartments of a simple cell. *Proc Natl Acad Sci U S A.* 2001;98:13049–13054.
47. Lugnier C, Keravis T, Le Bec A, Pauvert O, Proteau S, Rousseau E. Characterization of cyclic nucleotide phosphodiesterase isoforms associated to isolated cardiac nuclei. *Biochim Biophys Acta.* 1999;1472:431–446.
48. Okruhlicova L, Tribulova N, Eckly A, Lugnier C, Slezak J. Cytochemical distribution of cyclic AMP-dependent 3',5'-nucleotide phosphodiesterase in the rat myocardium. *Histochem J.* 1996;28:165–172.
49. Boknik P, Neumann J, Schmitz W, Scholz H, Wenzlaff H. Characterization of biochemical effects of CGS 21680C, an A2-adenosine receptor agonist, in the mammalian ventricle. *J Cardiovasc Pharmacol.* 1997;30:750–758.
50. Lohse MJ, Benovic JL, Caron MG, Lefkowitz RJ. Multiple pathways of rapid beta 2-adrenergic receptor desensitization. Delineation with specific inhibitors. *J Biol Chem.* 1990;265:3202–3211.